

## Supporting information

### Forced phage uncorking: viral DNA ejection triggered by a mechanically sensitive switch

Miklós S.Z. Kellermayer, Zsuzsanna Vörös, Gabriella Csik and Levente Herényi

Department of Biophysics and Radiation Biology, Semmelweis University, Tüzoltó u. 37-47.,  
Budapest H-1094 Hungary

#### Measurement of T7 phage tail length

The length of the T7 phage tail was measured on height-contrast AFM images by drawing a linear section along the phage axis under visual control (**Fig. S1**). Tail length was measured as the distance, along this section, from the topographical inflection point, which marks the approximate location of the boundary between the capsid and the tail complex, to the tip of the tail. The distribution of tail lengths is shown in **Fig. S1.d**. We obtained a mean length of 22.8 nm ( $\pm 3.0$  nm,  $n = 149$ ).

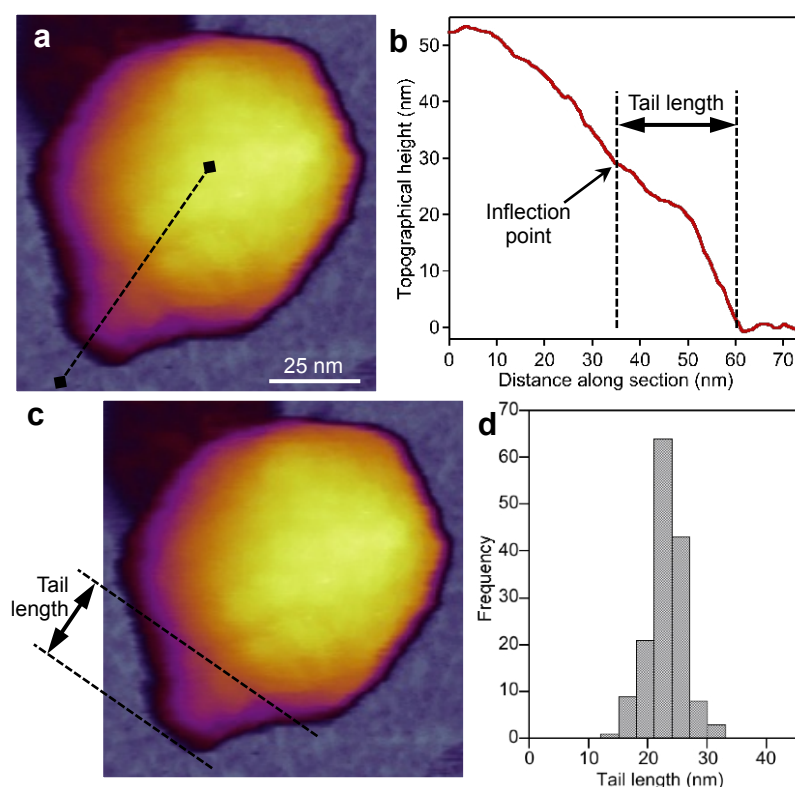


**Figure S1.** Measurement of T7 phage tail length. **a.** Height-contrast AFM image of a T7 phage. The dotted line drawn manually in the long axis of the phage, along the tail, marks the linear section along which topographical height data were collected. **b.** Topographical height as a function of distance along the linear section. Tail length was defined as the distance between the topographical inflection point and the very end of the tail. **c.** The tail-length definition projected onto the AFM image. **d.** Histogram of tail lengths.

## Estimating the dimensions of surface-adsorbed T7 DNA

The mean-square end-to-end distance of a statistical polymer chain equilibrated to a substrate surface may be calculated as<sup>1</sup>

$$\langle R^2 \rangle_{2D} = 4L_p L_C \left( 1 - \frac{2L_p}{L_C} \left( 1 - e^{-\frac{L_C}{2L_p}} \right) \right) \quad (S1)$$

In the limit of  $L_C \rightarrow \infty$ , equation (1) becomes

$$\langle R^2 \rangle_{2D} = 4L_p L_C \quad (S2)$$

Because the  $L_C$  of the T7 genome far exceeds the persistence length (nearly 300-fold), we used equation (S2) to calculate the theoretical end-to-end distance of the surface-equilibrated T7 dsDNA molecule. Considering the 13.6  $\mu\text{m}$  contour length ( $L_C$ ) of the T7 genomic DNA<sup>2</sup> and a 50 nm persistence length ( $L_p$ ) of dsDNA<sup>3</sup>, the mean end-to-end distance of the surface-equilibrated T7 DNA is expected to be  $\sim 1.6 \mu\text{m}$ . If an otherwise relaxed statistical polymer chain is driven to the surface rather than equilibrated to it, then the mean end-to-end distance of the chain will be smaller. In the extreme case the polymer chain is projected onto the surface. The mean-square projected end-to-end distance, in the limit of  $L_C \rightarrow \infty$ , can then be calculated as<sup>1</sup>

$$\langle R^2 \rangle_{proj} = \frac{1}{3} \langle R^2 \rangle_{2D} \quad (S3)$$

Given the above parameters of the T7 dsDNA, its projected end-to-end distance is expected to be  $\sim 0.9 \mu\text{m}$ . The area occupied by the surface-adsorbed full-length T7 dsDNA may be estimated with the help of the radius of gyration ( $R_G$ ), which is related to the end-to-end distance ( $R$ ) as

$$\langle R_G^2 \rangle = \frac{\langle R^2 \rangle}{6} \quad (S4)$$

Accordingly, the diameter of the circular area occupied by the T7 dsDNA is  $\sim 1.3 \mu\text{m}$  and  $\sim 0.7 \mu\text{m}$  for the surface equilibrated and surface-projected conditions, respectively. By comparison, the mean diameter of the area occupied by the ejected DNA measured in the AFM images was only 355 nm ( $\pm 57$  nm S.D.,  $n=43$ ) (**Fig. S2**).

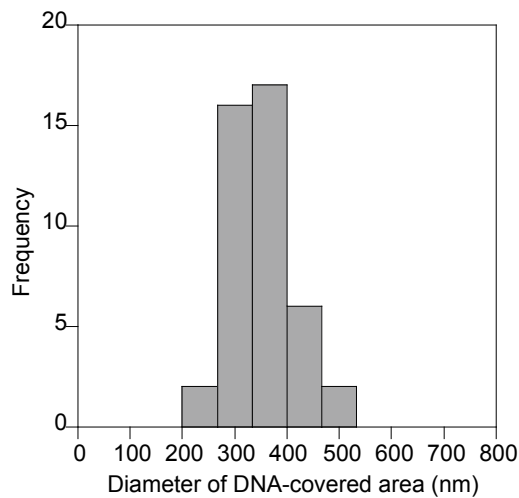


**Figure S2.** Distribution of the diameter of the area covered with T7 genomic DNA.

### Calculation of force exerted by the oscillating cantilever on the capsid

In order to calculate the average force on the capsid exerted by the oscillating cantilever, we carried out an empirical calibration procedure for each cantilever used. In this procedure the oscillating cantilever was pressed against a rigid control (mica) surface. Then the force was measured as a function of the detected cantilever oscillation amplitude. The stiffness-calibrated cantilever (Olympus BL-AC40TS-C2) was oscillated at its resonance frequency (20-27 kHz) by using photothermal excitation (BlueDrive™)<sup>4</sup> with a free amplitude of 100 mV, which corresponded to an amplitude of 2.5-3.5 nm depending on cantilever parameters. Stiffness calibration of the cantilever was carried out by using the thermal method<sup>5</sup>. The cantilever was moved with a constant rate (50 nm/s) towards the surface and both the average force and the oscillation amplitude (in terms of both position-sensor voltage and absolute distance) were measured. A calibration curve so obtained is shown in **Fig. S3**. By selecting an amplitude set-point for the feedback of the AFM imaging, we adjusted the average force, exerted by the cantilever on the capsid, between ~10 pN and ~40 pN. We note that because the cantilever tip is not interacting with the viral capsid throughout its oscillatory movement (i.e., the amplitude, in nanometers, is not equal to capsid distortion), the force acting on the capsid cannot be simply calculated from the amplitude and cantilever stiffness.

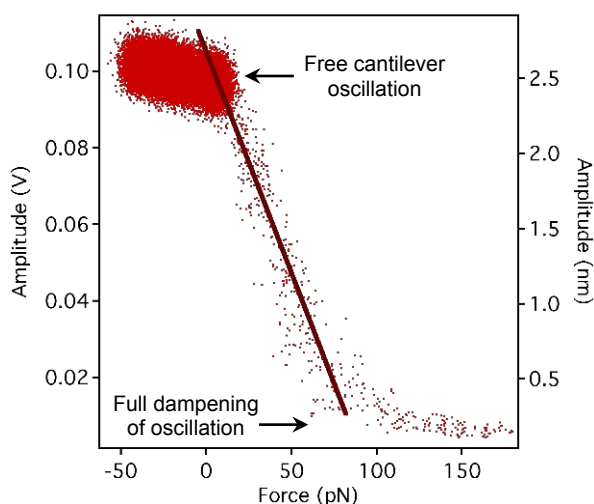


**Figure S3.** Calibration curve of the average cantilever force as a function of oscillation amplitude expressed either as position-sensor voltage (left axis) or absolute distance (right axis).

### Calculation of capsid pressure increment during AFM imaging

The pressure increment caused by indentation with the AFM cantilever may be calculated from the indentation force ( $F$ ), capsid stiffness ( $\kappa$ ) and the geometry of the capsid (**Fig. S4**).

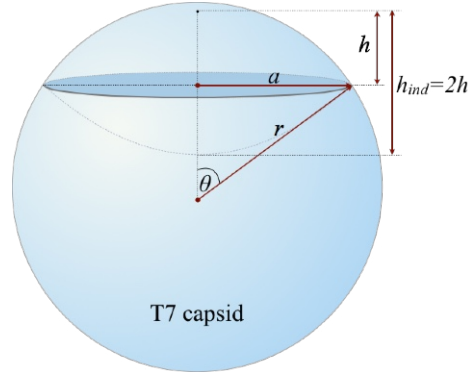


**Figure S4.** Schematics of T7 indentation with an AFM cantilever as a buckled sphere.

During AFM scanning, the tip of the cantilever indents the capsid shell with a distance ( $h_{ind}$ ) determined by the average indentation force and capsid stiffness as

$$h_{ind} = \frac{F}{\kappa} \quad (S5)$$

Considering, for example, an indentation force of 40 pN at the point of DNA release and a capsid stiffness<sup>6</sup> of  $0.7 \text{ Nm}^{-1}$ ,  $h_{ind}$  is 0.057 nm. Indenting the capsid reduces its volume by twice the spherical section (**Fig. S4**) which can be calculated from the indentation distance ( $h_{ind}=2h$ ) and the capsid radius ( $r$ ) as

$$V_{\Delta} = \frac{2\pi}{3} h^3 (3r - h) \quad (S6)$$

Taking the above indentation distance and considering a capsid radius of  $30 \text{ nm}$ <sup>7</sup>,  $V_{\Delta}$  is  $0.153 \text{ nm}^3$ . Assuming the T7 capsid to be a sphere, its volume ( $V_C$ ), calculated as

$$V_C = \frac{4}{3} \pi r^3 \quad (S7)$$

is  $1.13 \times 10^5 \text{ nm}^3$ . Accordingly, indentation causes a nearly negligible ( $1.35 \times 10^{-6}$ -fold) reduction in capsid volume at the maximum of cantilever deflection. The resulting pressure increment may be calculated from compressibility ( $\beta$ ) as

$$\Delta p = \frac{1}{\beta} \frac{\Delta V}{V_C} \quad (S8)$$

Considering a compressibility range of  $1 \times 10^{-10} - 2 \times 10^{-10} \text{ Pa}^{-1}$  measured for globular proteins in water<sup>8</sup>, the imposed pressure change is 6.75 - 13.5 kPa (0.0675 - 0.135 atm, which is between  $\sim 0.1$  and  $\sim 0.2$  % of the pressure assumed to be present in the DNA-filled capsid (60 atm)<sup>9</sup>.

### Measuring the rate of T7 DNA ejection under mechanical load

We calculated the rate of force-driven DNA ejection by counting the number of capsids, within an AFM image of a large sample area, that ejected their DNA as a result of exposure to mechanical force. The force-dependent rate ( $k_F$ ) was calculated according to

$$k_F = \frac{1}{t_r} \frac{N_{ejected}}{N_{total}} \quad (S9)$$

where  $t_r$  is the average residence time of the cantilever on a capsid, and  $N_{ejected}$  and  $N_{total}$  are the numbers of capsids which ejected their DNA and the total number of capsids within the image,

respectively.  $t_r$  was calculated from image parameters (**Fig. S5**) with the consideration that the binarized image area of a capsid corresponds to the time the AFM cantilever was residing on its surface.

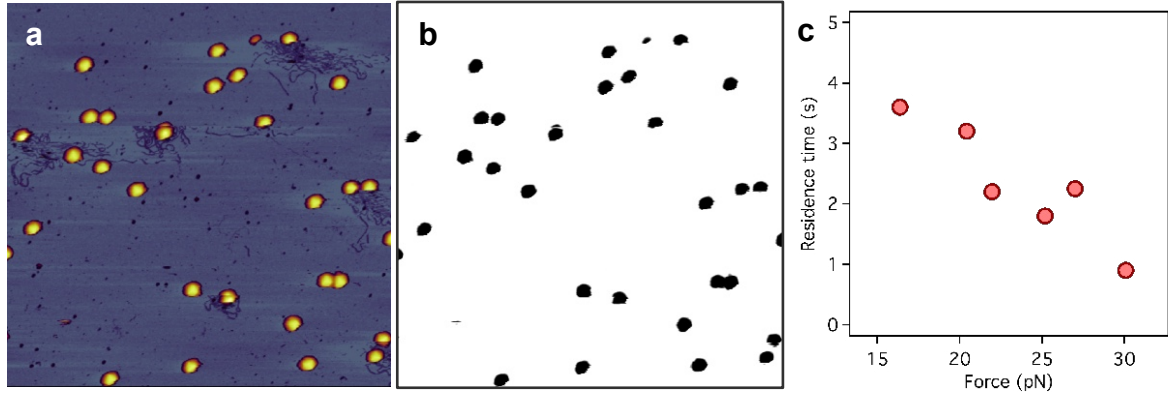


**Figure S5.** Calculation of the residence time of the cantilever on a capsid. **a.** Original height-contrast AFM image. **b.** Binary image of **a.** **c.** Residence time, calculated from the image particle areas, as a function of mechanical force.

Based on the AFM scan rate (0.22 Hz typical in these experiments) and the number of image pixels per line (512) one pixel corresponds to 8.9 ms. From the area, in pixels, of a binarized T7 capsid, the residence time of cantilever interaction can then be calculated. The area was counted twice to account for both the forward and backwards scanning. The decrease of residence time seen as a function of increasing loading forces (**Fig. S5.c**) reflects the progressively increasing image compression of the surface-adsorbed particles. Importantly, the rate of ejection calculated here refers to the rate of the triggering process, and it is not analogous to the speed at which DNA is expelled during ejection.

If mechanical force ( $F$ ) accelerates a reaction, then the reaction rate ( $k_F$ ) is increased relative to the spontaneous, thermally activated one ( $k_0$ ) because the activation energy ( $E_a$ ) is decremented with a mechanical energy component ( $F\Delta x$ ) according to

$$k_F = Ae^{-\frac{E_a - F\Delta x}{k_B T}} = Ae^{-\frac{E_a}{k_B T}} e^{\frac{F\Delta x}{k_B T}} = k_0 e^{\frac{F\Delta x}{k_B T}} \quad (\text{S10})$$

Here  $A$  is the pre-exponential factor or, within the framework of the transition-state theory, the attempt frequency that sets the rate of collisions. The theoretical maximum of  $A$  is determined by the thermal energy ( $k_B T$ ) and Planck's constant ( $h$ ) as

$$A = \frac{k_B T}{h} \quad (\text{S11})$$

where  $k_B$  is Boltzmann's constant and  $T$  is absolute temperature. At the typical temperature used in our experiments (20 °C) the value of  $A$  is  $6 \times 10^{12} \text{ s}^{-1}$ . In equation S10  $\Delta x$  is the distance, along the reaction coordinate, between the initial state of the system and the transition state of the reaction. Fitting equation S10 (hence equation 1 of the main text) to the  $k_F$  versus  $F$  plot (**Fig. 3.d**) allows the estimation of  $k_0$  and  $\Delta x$ , which are coefficients of the non-linear fitting procedure. Based on our data we obtained  $2.6 \times 10^{-5} \text{ s}^{-1}$  ( $\pm 2.7 \times 10^{-5} \text{ s}^{-1}$ ) and 1.2 nm ( $\pm 0.1 \text{ nm}$ ) for  $k_0$  and  $\Delta x$ , respectively. We note that the spontaneous triggering rate is non-zero; indeed, we observed a progressive increase of spontaneously ejected DNA as a function of time in our AFM experiments. After three hours of incubation the number of capsids having ejected their DNA increased above 10 %. We also note that the error of the calculated spontaneous rate is

large and comparable to the value itself. There are several factors that may contribute to the error beyond the stochastic nature of the process, including geometric constraints related to the binding and orientation of the capsids on the substrate surface and variation in the momentary force acting on the capsids. It is also important to note that, because of cantilever oscillation, force changes sinusoidally as a function of time, but the calculations above apply to the average forces obtained from the empirical calibration (**Fig. S3**). Because force is in the exponent (see equation S10), very high DNA-triggering rates may be induced, although only for brief periods of time, at the peak of the force oscillation. From  $k_0$  the activation energy can be calculated with the above constants and parameters as

$$E_a = k_B T \ln \left( \frac{A}{k_0} \right) \quad (\text{S12})$$

Thus we obtain 23 kcal/mol for  $E_a$ , which compares well with the range of 20-40 kcal/mol found in bulk experiments for the initial steps of viral DNA ejection<sup>10</sup>.

### Finding the center of mass of ejected and surface-adsorbed DNA

The center of mass of the ejected and surface-adsorbed DNA molecule can be obtained by using image processing methods (**Fig. S6**). First the phase-contrast AFM image was converted to grayscale image (**Fig. S6.a**), then inverted. To exclude the contribution of the capsid image to the calculation, the pixels corresponding to the capsid were erased and converted to the background (**Fig. S6.b**). The center of mass was calculated as the pixel value-weighted centroid by using the built-in algorithm of the ImageJ program.

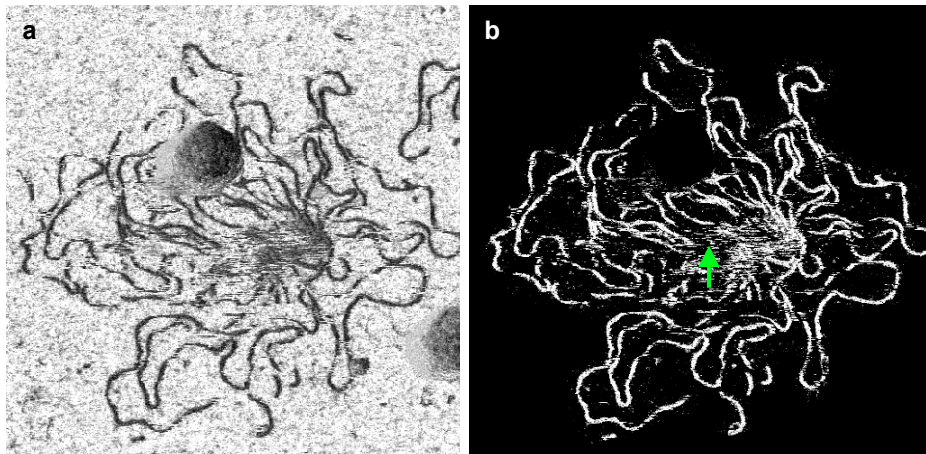


**Figure S6.** Calculation of the center of mass of the ejected and surface-adsorbed DNA molecule based on image properties. **a.** Phase-contrast AFM image converted to grayscale. **b.** Image after inversion and removal of the capsid pixels. The calculated center of mass is indicated with the green arrow.

### Estimating the density distribution of ejected and surface-adsorbed DNA

To estimate the spatial density of DNA strands within the image, local pixel averaging was carried out by convolution with a large (49×49) Gaussian kernel (**Fig. S7**).

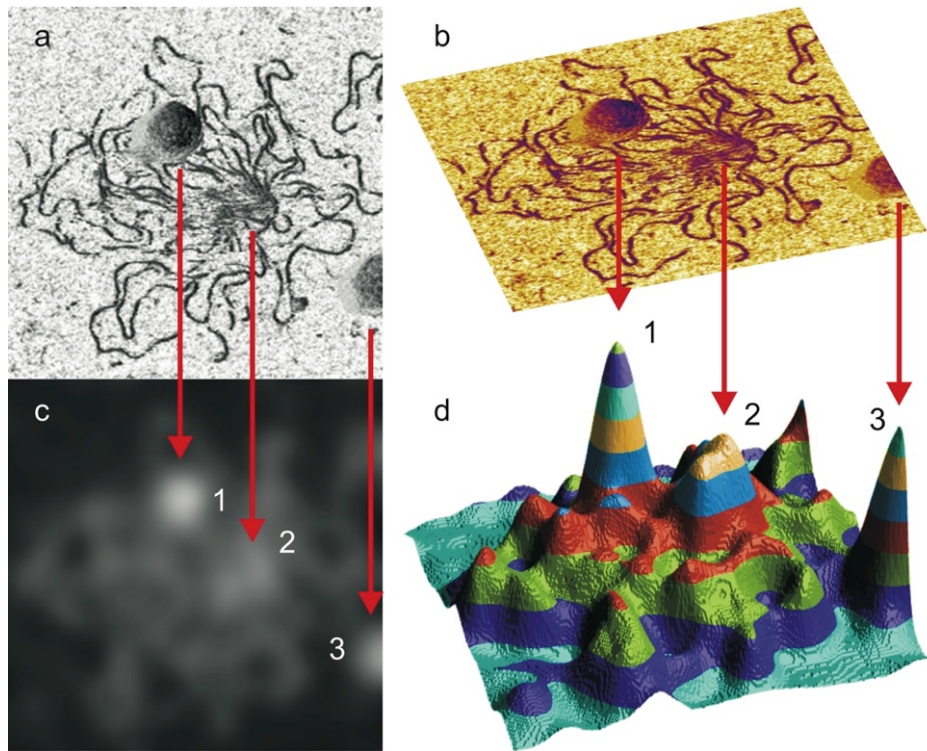


**Figure S7.** Finding the centers of density. **a.** Phase-contrast AFM image of a T7 phage particle that ejected its DNA. **b.** Same image tilted to correlate with the surface map. **c.** AFM image after filtering with Gaussian kernel. Numbers indicate density maxima. **d.** Surface map of the filtered image.

### Characterization of ejected globular particles

The globular particles observed on the mica surface in the vicinity of the ejected DNA were analyzed for their topographical height so as to estimate their dimensions (**Fig. S8**). We note that the diameter of the particles is inflated in the AFM images due to tip convolution, therefore the height provides a better estimate of the particle size. The diameter of the ejected dsDNA molecule, measured from its topographical height is  $\sim 2$  nm, which compares well to its known structure. The mean size of the globular particles, measured as their topographical height, is  $5.0$  nm ( $\pm 1.5$  nm S.D.,  $n=81$ ).

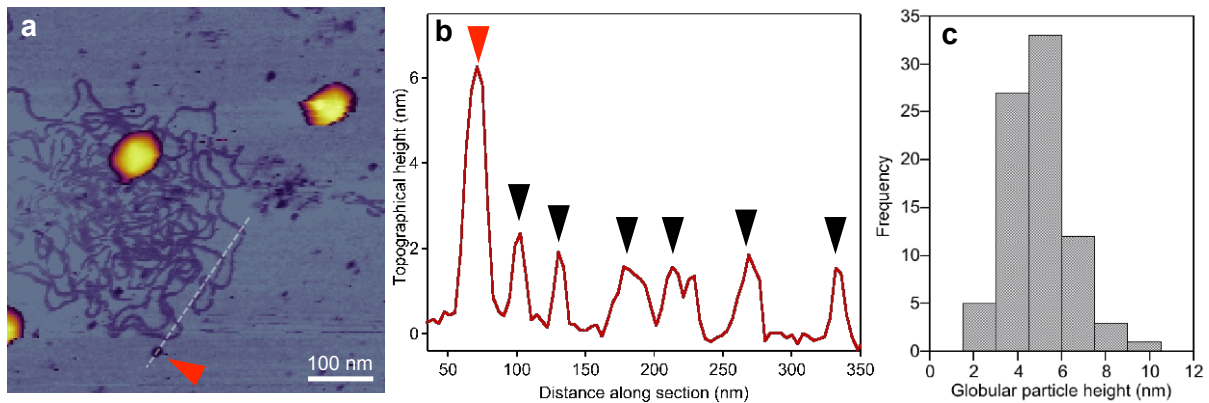


**Figure S8.** Measurement of the topographical height of globular particles observed in the vicinity of phages that have ejected their DNA. **a.** Height-contrast AFM image showing T7

phages, one of which has ejected its dsDNA (figure identical to **Fig.4.b** of the main text except for the white dotted line). White dotted line marks a linear section along which the topographical height distribution was measured. Red arrow points at a globular particle near the ejected DNA molecule. **b.** Topographical height as a function of distance along the demarcated section. Black arrows point at the sites where the section crossed the dsDNA molecule. Red arrow points at the topographical contour of the globular particle. **c.** Height distribution of globular particles.

### **Exploring the possibility of mechanically-induced structural damage to the tail complex**

It is a plausible possibility that the mechanically-triggered DNA ejection might be caused by the cantilever tip directly breaking the tail off the capsid. We tested for this possibility with two types of measurements. In the first (**Fig. S9**), we systematically avoided mechanically touching the tail, and exposed the body of the capsid to progressively increasing forces. We measured, by detecting DNA trapped on the surface, whether DNA became ejected during such a partial capsid tapping. In the second type of test (**Fig. S10**) we simply surveyed whether viruses that have ejected their DNA during AFM scanning displayed significant changes in the topographical structure of their tail.

We observed that it was possible to trigger the ejection of DNA by tapping the body of the capsid, without touching the tail. An example image sequence shown in **Fig. S9** (see also **Supplementary video 2**) clearly demonstrates that partial tapping of the T7 capsid body leads to the ejection of DNA. Furthermore, the subsequent imaging of the entire virus shows that the conical tail structure remained in its position, indicating that tail breakage is not the reason for DNA release.

We also show a series of images (**Fig. S10**) which indicate that the conical structure of the tail is maintained in spite of the fact that the virus has ejected its DNA. The conical shape is particularly well observable in the 3D-rendered AFM image of a T7 virus, the tail of which points away from the surface (**Fig. S10.e**). Although internal structural changes, which are unresolvable by topographical analysis, may have occurred in the tail, it seems clear that breaking the tail completely off the capsid is not the mechanism of mechanically-triggered DNA ejection. While it is difficult to exclude the possibility that DNA may leave the capsid through cracks in between the capsomeres, the large quantities of DNA ejected from the capsids in our experiments have most likely left via the natural pathway, through the tail.

The statistics of the structural appearance of the tail in T7 capsids that ejected their DNA is shown in **Fig. S11**. The topological tail structure was partitioned, by visual evaluation, into three groups: missing, shrunk and conical. Less than 10 % of the capsids analyzed had missing tails, and the capsids that had either shrunk or conical (i.e., more or less intact) tails were similar. We have not been able to identify phage particles with significantly extended tails. A tail extension, formed by core proteins, is thought to build up the DNA ejection conduit in T7.<sup>11</sup> Conceivably, under *in vitro* conditions the process proceeds *via* slightly different steps than *in situ*, in the bacterial cell wall. Possibly, the presence of the bacterial wall components assist in the formation of the tail extension. In lieu of the bacterial wall, the ejected core proteins might simply diffuse away, and the conformationally altered tail complex might lose some of its parts, thereby resulting in a shrunk topographical appearance.

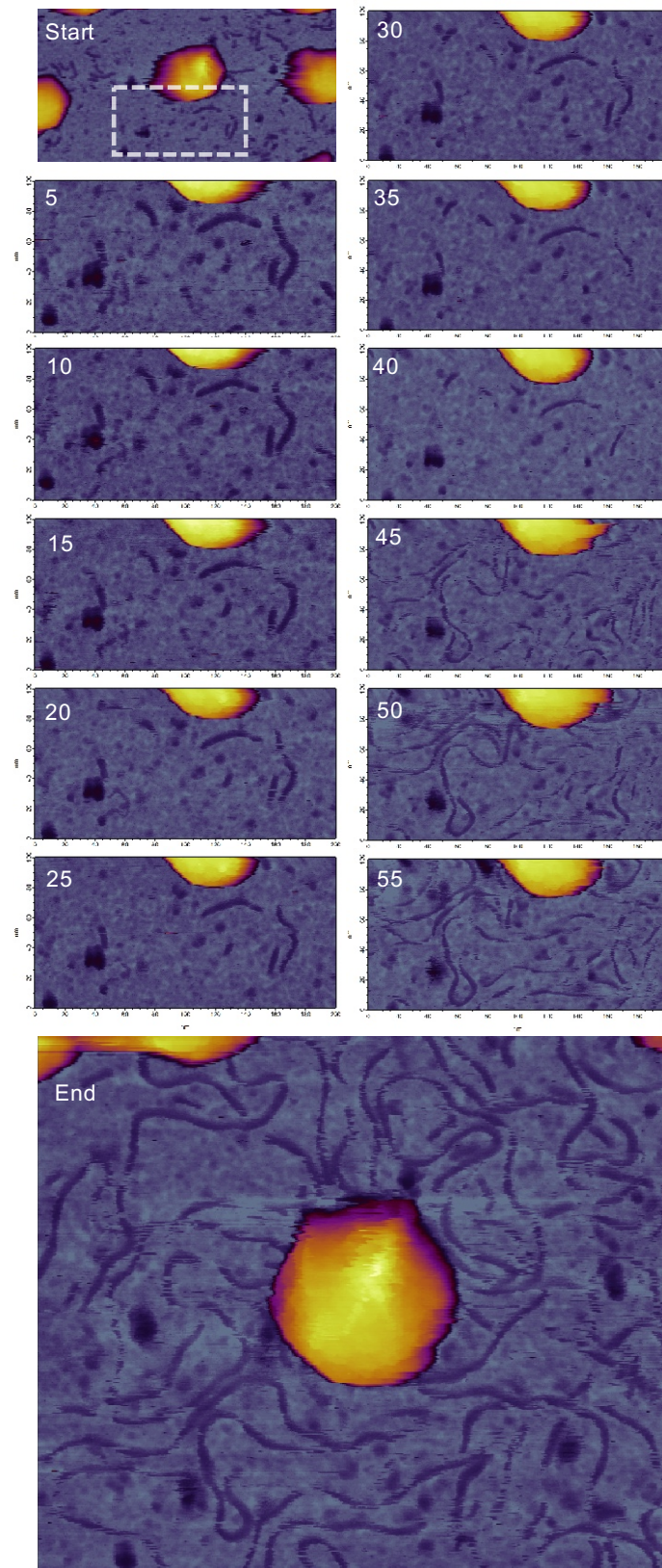


**Figure S9.** DNA ejection during partial scanning of the T7 bacteriophage. Temporal sequence of images are shown. The images are separated by 5 minutes. The boxed area in the starting image was scanned repetitively with progressively increasing forces (lowered setpoint). The bottom image labeled "End" shows the same T7 capsid following the partial tapping experiment. See also **Supplementary video 2**.

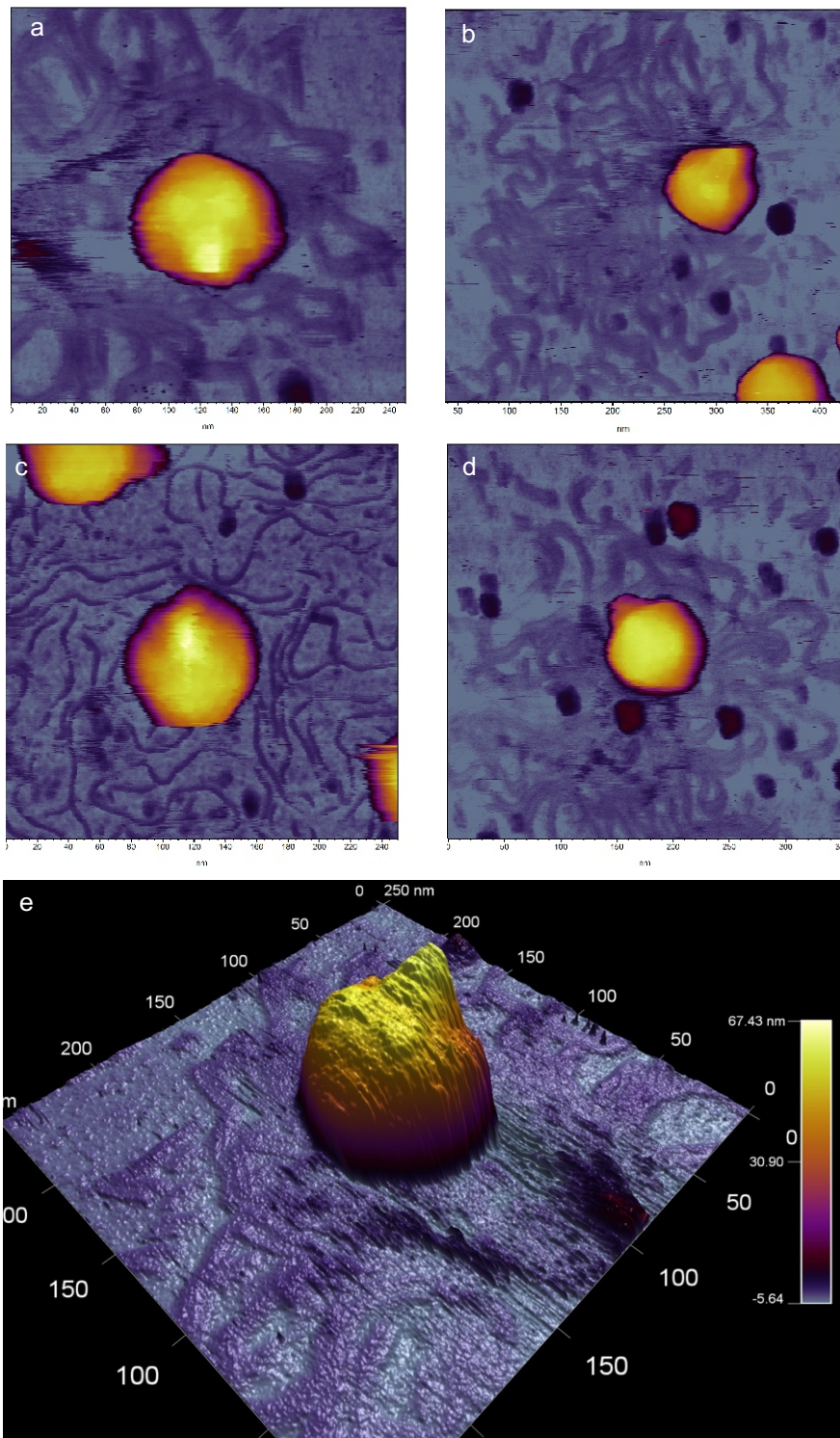


**Figure S10.** Examples of T7 phages from which DNA was ejected during AFM scanning.

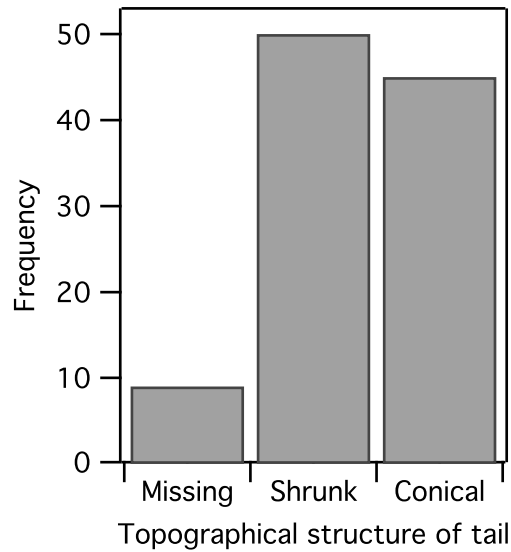


**Figure S11.** Statistics of T7 capsids that ejected their DNA according to the topographical appearance of the tail.

### **Orientational symmetry of the T7 capsids**

We carried out an analysis of the orientational symmetry of the T7 capsids that ejected their DNA. More than 55% of the capsids displayed three-fold symmetry, 44% two-fold symmetry, and we found only one capsid that we judged as to display five-fold symmetry. The statistics reflect the orientational distribution of the capsids on the mica surface, and there appeared no orientational preference of the capsids from which DNA was ejected upon mechanical trigger.

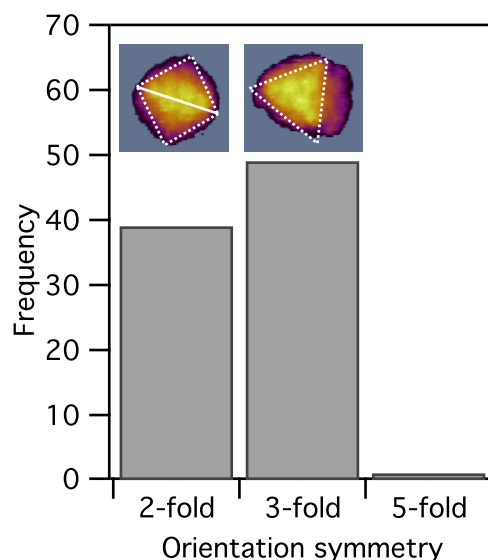


**Figure S12.** Statistics of T7 capsids that ejected their DNA according to their orientational symmetry. **Insets** show examples of T7 capsids in two- and three-fold symmetric arrangements. The dotted lines guide the eye so that the orientation symmetry may be easily identified.

## Supplementary video 1

Video sequence assembled based on *in situ* AFM images of a T7 phage particle ejecting its genomic DNA. Each frame was collected in 8.7 minutes with a line-scan frequency of 0.97 Hz. Sequential up-and-down scans were collected. The first frame of the video was collected in a downward scan. Left panel shows the height contrast, whereas the right panel the phase contrast image sequence.

## Supplementary video 2

Video sequence showing the partial tapping of a T7 capsid. Following the initial, gentle AFM scan the selected T7 particle was repetitively scanned with increasing forces so that only the lower part of the capsid body was tapped and the conical tail was left unperturbed. Please, note that ejected DNA appears in the 9th frame of the partial scan. Finally, the entire capsid was re-scanned to observe any changes in the overall capsid structure. The movie was assembled based on **Fig. S9**.

## References

- 1 C. Rivetti, M. Guthold and C. Bustamante, *J Mol Biol*, 1996, **264**, 919–932.
- 2 M. E. Cerritelli, N. Cheng, A. H. Rosenberg, C. E. McPherson, F. P. Booy and A. C. Steven, *Cell*, 1997, **91**, 271–280.
- 3 S. B. Smith, Y. Cui and C. Bustamante, *Science*, 1996, **271**, 795–799.
- 4 A. Labuda, J. Cleveland and N. A. Geisse, *Microscopy and Analysis (Euro)*, 2014, **28**, S21–S25.
- 5 J. L. Hutter and J. Bechhoefer, *Review of Scientific Instruments*, 1993, **64**, 1868–1873.
- 6 Z. Vörös, G. Csik, L. Herényi and M. S. Z. Kellermayer, *Nanoscale*, 2017, **9**, 1136–1143.
- 7 G. Rontó, M. M. Agamalyan, G. M. Drabkin, L. A. Feigin and Y. M. Lvov, *Biophysj*, 1983, **43**, 309–314.
- 8 D. P. Kharakoz, *Biophysj*, 2000, **79**, 511–525.
- 9 D. E. Smith, S. J. Tans, S. B. Smith, S. Grimes, D. L. Anderson and C. Bustamante, *Nature*, 2001, **413**, 748–752.
- 10 I. J. Molineux and D. Panja, *Nat. Rev. Microbiol.*, 2013, **11**, 194–204.
- 11 B. Hu, W. Margolin, I. J. Molineux and J. Liu, *Science*, 2013, **339**, 576–579.